# Particle-in-cell Simulations of Potential Structure around Electric Solar Wind Sail Tethers

**IEPC-2015-298／ISTS-2015-b-298**

*Presented at Joint Conference of 30th International Symposium on Space Technology and Science, 34th International Electric Propulsion Conference and 6th Nano-satellite Symposium*
*Hyogo-Kobe, Japan*
*July 4–10, 2015*

Kento Hoshi*, Hirotsugu Kojima† and Hiroshi Yamakawa‡
*Kyoto University, Kyoto, Kyoto, 611-0011, Japan*

**Abstract: In this paper, we perform the first three dimenstional particle-in-cell simulations of the electric solar wind sail, which is recently proposed new propulsion system. We investigate the potential structure around the tethers of the electric solar wind sail and estimate the effect on thrust characteristics of them. The potential becomes asymmetric between in sunward side and in sunshade side. The potential distribution are slightly lower than that of the previous study, and the thrust characteristics may be decreased.**

## Nomenclature

| | |
|---|---|
| $F$ | = force |
| $j_{\mathrm{ph0}}$ | = current density of photoelectrons |
| $K$ | = propotional factor |
| $r_0$ | = length |
| $r_{\mathrm{w}}$ | = tether's radius |
| $\lambda_d$ | = debye length |
| $n_0$ | = background plasma density |
| $m_{\mathrm{p}}$ | = proton's mass |
| $v$ | = velocity |
| $V_0$ | = beam-accelerating potential |

*Ph.D student, Department of Electrical Engineering, kento_hoshi@rish.kyoto-u.ac.jp.
†Associate Professor, Research Institute for Sustainable Humanosphere.
‡Professor, Research Institute for Sustainable Humanosphere.

# I. Introduction

An electric solar wind sail is a new propulsion system recently proposed by Janhunen,[1] which consists of several-kilometre long, thin, conducting tethers. Tethers are kept at a high positive electrical potential on the order of several kilo-volts with an electron gun. The positively charged tethers deflect the momentum of solar wind protons, so that the tethers obtain a propulsive force. The system requires only electron sources and electrical power to generate thrust, hence it is expected to be a propellantless space propulsion.

Its thrust characteristics are not clear at present. Janhunen and Sandroos performed the one-dimenstional test particle simulation to estimate the potential structure around the tether, and performed the two-dimenstional particle-in-cell (PIC) simulations to evaluate the force acting on the tether in 2007.[2] The force per unit length acting on the sail found by them is given by

$$\frac{\mathrm{d}F}{\mathrm{d}z} = \frac{K m_p n_0 v^2 r_0}{\sqrt{\exp\left[\frac{m_p v^2}{eV_0}\ln\left(\frac{r_0}{r_w}\right)\right] - 1}} \tag{1}$$

where $z$ is the axis along the tether, $K$ is a propotional factor ($\sim 3.09$ obtained from their Monte Carlo simulation), $m_p$ is the proton's mass, $n_0$ is the electron density, $v$ is the drift velocity of solar wind, $r_0$ is the debye length, $V_0$ is the tether's electrical potential, $r_w$ is the tether radius. Succeceful and efficient mission trajectory in the solar system was calculated using the analytic expression.,[3] and more precise thrust modeling considering ion-scattering are studied.[4]

In addition, Janhunen proposed the thrust may become at most 5 times larger than that estimated from Eq.(1) due to trap and reduce electrons around the tether by using 1-D test particle simulations.[5]

In these previous studies, the electrical potential of tethers are fixed to tens of kilovolts, and do not vary in calculation. Background electrons and ions impacting are ignored because the wires are assumed very thin. However, the positive electrical potential is induced by electron beam emission from the edge of the tether in practise. In addition, photoelectrons are also emitted from their surface despite the tether is thin. These electrons emitted from the tether itself effect on the potential structure around them, and the thrust characteristics may be change.

In this paper, we perform the first three-dimensional particle-in-cell simulations of the long tethers in solar wind environment with no assumption of biased the tether's potential. We show the electric potential structure and plasma densities around the tether. Comparing our results with the 1-D plasma simulation results in previous study, we estimate the effect on the thrust performance of the electric solar wind sail.

# II. Simulation Settings

To calculate the spacecraft charging numerically, we use the simulation code called HiPIC, which was developed by the Japan Aerospace Exploration Agency's Engineering Digital Innovation Center (JEDI).[6] HiPIC has 3-D rectangular grids and uses the full PIC method for calculating collision-less kinetic plasma. We solve Newton's equations of motion for each particle by using Buneman-Boris method, and solve Poisson's equations for obtaining an electric potential distribution in the computational domain by using discreate sine transformation. HiPIC calculate an interaction between plasmas and the spacecraft model, which is modeled as a rectangular internal boundaries. If charged particles impact the tether's surface, their charges accumulate on the surface and contribute to the electric potential of the tether. The tether is located on the center of the computational domain as shown in Fig. 1. The surface potential of the spacecraft is initially set to 0 V.

The background plasma in solar wind environment is assumed. Electron's and proton's density are set to $n_0 = 10\,/\mathrm{cc} = 1.0 \times 10^7\,/\mathrm{m}^3$, their temperature are set to $k_B T_e = k_B T_i = 12\,\mathrm{eV}$, and they has the drift velocity $v = 400\,\mathrm{km/s}$ towards x-axis. The background plasma particles are inject from all the domain boundaries in each time step. The magnetic field is assumed as zero, not considering the interplanetary magnetic field (IMF) because it is very small value and ignorable for the particle's motion. Photoelectrons are emitted from the tether's surface with their current density $j_{\mathrm{ph}0} = 14.4\,\mathrm{A/m}^2$, towards the sun ($x = 0$). Secondary electrons are neglected in these simulations, because they are returned to tether's surface if the tether's potential is higher than +10 V.[7]

In order to simulate active charging, an electron beam is emitted from the edge of the surface, $(x, y, z) = (127.5, 356.0, 127.5)$, as shown in Fig. 1. The accelerating potential of an electron beam is set to 50 V and

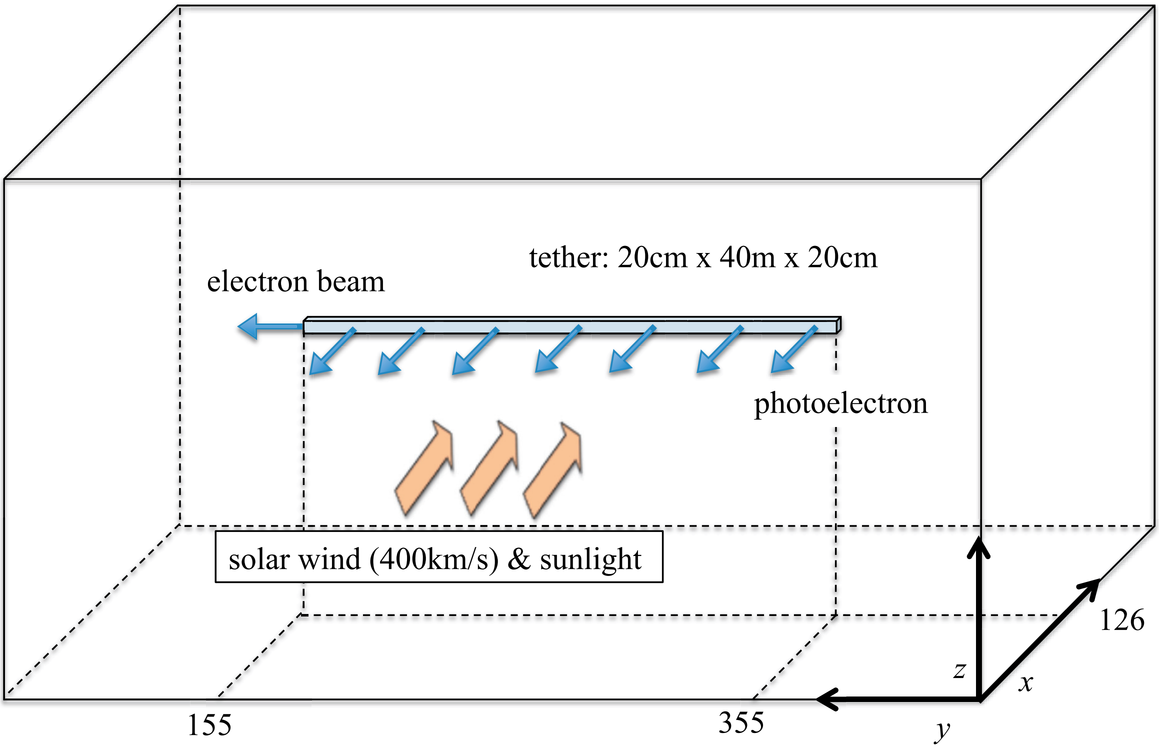


**Figure 1. Definition of the tether model and plasma environment. Background plasmas have solarwind velocity along $x$-axis. Photoelectrons are emitted towards solarwind. Electron beam is emitted along $y$-axis from the edge of the tether.**

**Table 1. Simulation Parameters**

| Parameter | Value |
|---|---|
| Background plasma spiecies | Electron, Proton |
| Background plasma density | 10/cc ($= 10^7$ /m$^3$) |
| Background plasma temperature | 12.0 eV, Maxwellian |
| Drift velocity of background plasma | 400 km/s |
| Debye length | 8. m |
| Magnetic field | None |
| Photoelectron current | 14.4 A/m$^2$ |
| Photoelectron temperature | 2.0 eV |
| Electron beam temperature | 0.1 eV, (Drift–Maxwellian) |
| Electron beam emission radius | 5.0 cm |
| Time step width | 10 ns |
| Grid spacing | 0.2 m |
| System length | 51.2$x$102.4$x$51.2 m (256x512x256 grids) |
| Boundary conditions | $V = 0$ V at edges of the system. |

the beam current is set to 100 $\mu$A. The electric potential of the surface rises up after the beam emission starts and converges at a beam-accelerating potential.[7] We summarize the parameters that are used in this simulation in Table. 1.

We performed simulations on these conditions and evaluated the potential structure around the tether surface. Note that the tether's radius in our simulations (= 10 cm) are much larger than the proposed radius ($\simeq 0.1\,\mu$m).[1] due to technical difficulty of simulations. But both radius are smaller than the debye length ($\lambda_d = 8.14$ m), so this condition will not cause a significant difference.

## III. Results and Discussion

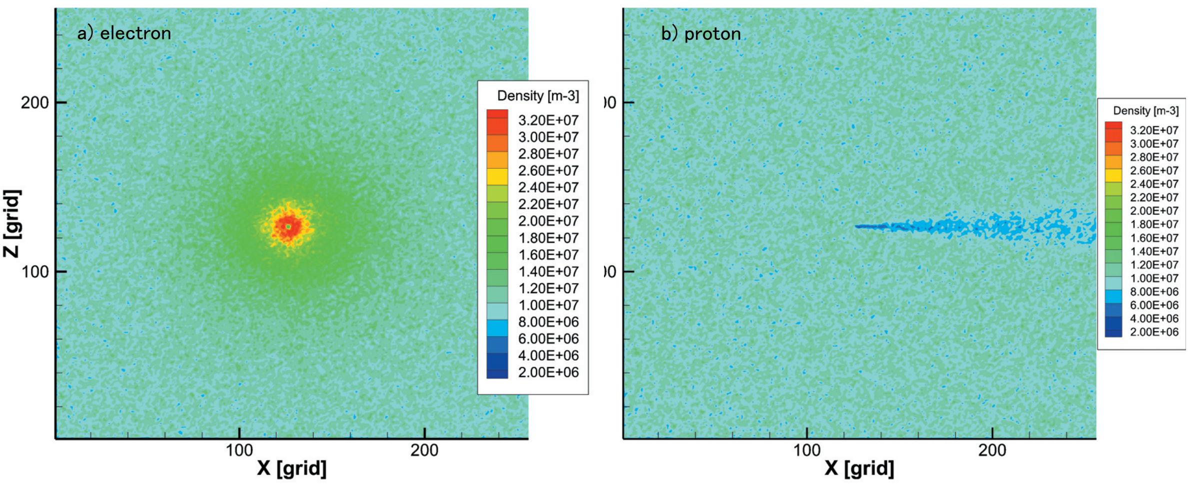


**Figure 2. Density distribution of background plasmas. a) Background electron density. b) Background proton density. Electron are accumulated around the tether attracted by the tether's potential. Proton are deflected by the potential and decreased behind the tether.**

Fig. 2 shows the background plasma's density distribution. Fig. 3 shows the 3-D potential distribution around the tether, the slices at $x = 127.5$ and $y = 157.0, 256.0, 349.0$. Fig. 4 shows the 1-D potential distribution at $z = 127.5$, and $x = 127.5$ of $y$-slices in Fig. 3.

Proton's density behind the tether become smaller than the nominal value ($n_0 = 10$/cc). In contrast,

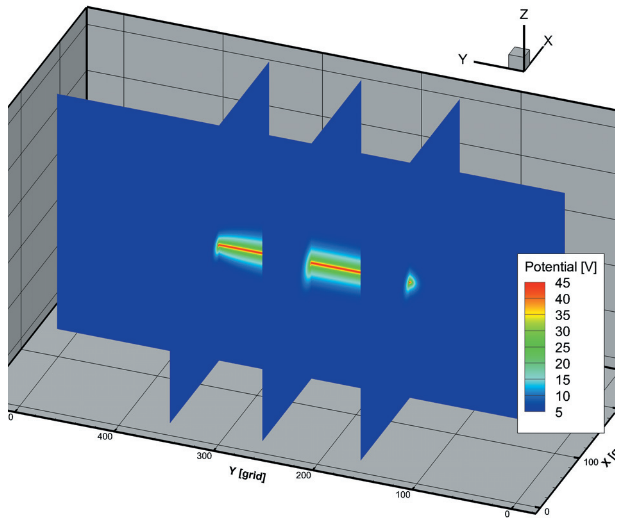


**Figure 3. Potential distribution around the tether. The slice on $x$-axis is at $x = 126.5$, the slices on $y$-axis are $y = 157, 256, 349$ respectively.**

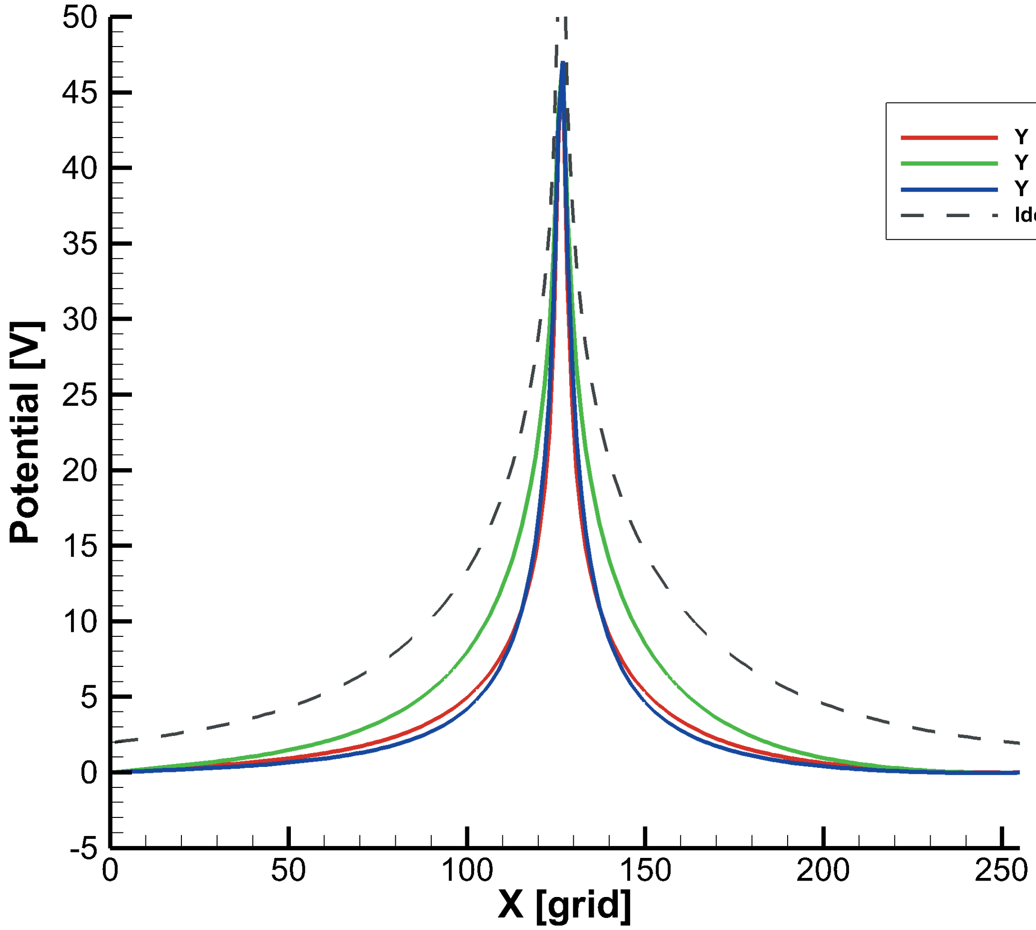


**Figure 4. Potential distribution along $x$-axis. Solid lines show the slices at $z = 127.5$ of the slices in the above Fig. 3. The dotted line show the ideal potential distribution studied by Janhunen and Sandroos.[2]**

electrons accumulated around the tether and they do not show the asymmetricity in sunward side and in sunshade side. The tether's electrical potential becomes 45 V, similar to the beam-accelerating potential.

A typical potential distribution may be similar to the green line in Fig. 4 because $y = 256$ is the center of the tether.

The positive spacecraft potential attracts electrons from sunward, and then the electrons move towards the tether. However, the tether is thinner than the debye length (8 m on these conditions), so that almost all of background electrons cannot impinge on the tether's surface. They pass by the tether and accumulate in the shade side of the tether, in contrast to proton's decreasing in the shade side.

Furthermore, the red and blue solid lines ($y = 157$, and 349) in Fig. 4 shows the potential around an electron emission point. The electric potential become slightly lower than other lines due to returning beam elecrons. An arrangement of electron guns along the tether have not been considered at presend. If many electron guns are required to maintain the surface potential in practise, the potential decreasing may affects the thrust characteristics.

In previous study, the potential around the tether was asummed by Eq. (2).[2]

$$V(r) = \frac{V_0}{2} \frac{\ln\left[1 + (r_0)/r^2\right]}{\ln(r_0/r_w)} \tag{2}$$

The dotted lines in Fig. 4 shows Eq. 2, where $V_0 = 50\,\mathrm{V}, r_\mathrm{w} = 0.2\,\mathrm{m}, r_0 = 16.28\,\mathrm{m}(= 2\lambda_d)$. Our simulation results (solid lines) are significantly lower ($\simeq 50\,\%$) than that of the previous study.

The thrust characteristics are formularized from the dotted line, Eq. (2). Hence, the thrust of the solar wind sail may be lower within more realistic potential distribution. The thrust model should be improved with the modification of the potential distribution. If the decreasement of the potential obtained from our simulations are correct in $V_0 = 20\,\mathrm{kV}$ case, the thrust becomes half as much as the conventional model, that is, $10 - 15\,\mathrm{nN/m}$.

## IV. Conclusion

In this paper, we have performed the first 3-D Particle-in-cell simulations of the electric solar wind sail. Our simulations calculated an electron beam emission from the edge of tether, and charged particles impinging on the surface, both have not been considered in previous studies. We have shown the electric potential distribution and density distribution around the tether . The potential are $\simeq 50\,\%$ lower than that of the previous study. If the decreasement of the potential obtained from our simulations are correct in $V_0 = 20\,\mathrm{kV}$ case, the thrust might become $10 - 15\,\mathrm{nN/m}$, which is half times as much as that of the conventional thrust model. Our future tasks are to find an analytical expression of thrust characteristics to correspond our 3-D PIC simulations.


## Acknowledgments

The computations in the present study were performed using the KDK system in the Research Institute for Sustainable Humanosphere (RISH) at Kyoto University. The present study was supported by JSPS KAKENHI Grant Number 50260013.


## References


[1]Janhunen, P., "Electric sail for spacecraft propulsion," *Journal of Propulsion and Power*, Vol. 20, No. 4, 2004, pp. 763–764.

[2]Janhunen, P. and Sandroos, a., "Simulation study of solar wind push on a charged wire: basis of solar wind electric sail propulsion," *Annales Geophysicae*, Vol. 25, No. 3, 2007, pp. 755–767, doi:10.5194/angeo-25-755-2007.

[3]Mengali, G., Quarta, A. a., and Janhunen, P., "Electric Sail Performance Analysis," *Journal of Spacecraft and Rockets*, Vol. 45, No. 1, 2008, pp. 122–129, doi:10.2514/1.31769.

[4]Sanchez-Torres, A., "Propulsive Force in an Electric Solar Sail," *Contributions to Plasma Physics*, Vol. 54, No. 3, 2014, pp. 314–319, doi:10.1002/ctpp.201410077.

[5]Janhunen, P., "Increased electric sail thrust through removal of trapped shielding electrons by orbit chaotisation due to spacecraft body," *Annales Geophysicae*, Vol. 27, No. 8, 2009, pp. 3089–3100, doi:10.5194/angeo-27-3089-2009.

[6]T. Muranaka, and I. Shinohara, and I. Funaki, and Y. Kajimura, and M. Nakano, and R. Tasaki, "Research and development of plasma simulation tools in JEDI/JAXA," *Journal of Space Technology and Science*, Vol. 25, 2011, pp. 1–18.

[7]Lai, S. T., *Fundamentals of spacecraft charging: spacecraft interactions with space plasma*, Princeton University Press, 2011.